



## Synthesis and Adsorption Study of some Chitosan Acidic Derivatives as Dispersants for Ceramic Alumina Powders



Eman S. Al-Allaq, Hadi S. Al-Lami and Ali H. Al-Mowali

Department of Chemistry, University of Basrah, Basrah 61001, Iraq.

THE different functionality nature of chitosan adds to its application as a preferable natural polymer not only for the recovery, separation, and concentration of metal ions, but for the fabrication of a wide spectrum of efficient materials, and opens a new window to act as a dispersant for ceramic particles in an aqueous medium; this is why the current study focused on getting chitosan from chitin extracted from shrimp shells by known and modified chemical methods to obtain a high Degree of Deacetylation (DD) reached 93% to increase its solubility in a dilute acidic aqueous medium. Three acid chitosan derivatives were synthesized by grafting chitosan chains with glutaric, pimelic, and sebacic acids. The grafting process was checked by FTIR, which confirmed the compositions of the acid derivatives prepared as well as chitosan.

The ability of chitosan and its derivatives to act as a dispersant for alumina ceramics powder was assessed by sedimentation and rheological techniques. The results showed that they have good power for deflocculating alumina particles, this implies that they may be good dispersant for ceramic processing in aqueous media which is the priority for ceramic manufacturers.

The quantity of adsorbed dispersants,  $q_e$  (mg/g), was determined by thermal gravimetric analysis, and hence the remaining concentration in equilibrium  $C_e$  (mg/L), four different types of adsorption isotherm models were determined and evaluated by calculating the variables and constants for each type and studying the behavior of polymers prepared toward each model. The S-shape curve was obtained from plotting  $q_e$  vs  $C_e$  referring to that the adsorption follows BET isotherm of multilayer where each layer obeys Langmuir-Freundlich isotherm.

**Keywords:** Chitosan acid derivatives, Dispersant, Adsorption isotherm, Langmuir, Freundlich, BET, D-R.

### Introduction

Colloidal systems occur in a wide variety of situations. For instance, the flocculation of naturally occurring colloidal particles is of considerable importance in the formation of sediments, the sitting of river estuaries, agricultural soil conditioning, and the clarification of domestic water supplies. One of the most challenging problems in the study of colloidal systems is obtaining the desired stability and rheological properties of a suspension [1,2]. One usually makes use of dispersing agents to achieve

these properties that are of prime consideration in colloidal processing and are commonly regarded as the most important parameters to produce high quality, high-performance, and reliable ceramic products. The selection of an appropriate dispersant to optimize such properties is essentially dependent upon solvent characteristics, conformation process, and especially upon the physical-chemical characteristics of the ceramic powder and surface [3]. The confirmation of the adsorbed polymer is a major controlling factor in determining the stability of the dispersion of the mineral suspensions [4].

\*Corresponding author e-mail: [hadi.abbas@uobasrah.edu.iq](mailto:hadi.abbas@uobasrah.edu.iq)

Received 31/7/2019; Accepted 24/12/2019

DOI: 10.21608/ejchem.2019.15492.1940

© 2020 National Information and Documentation Center (NIDOC)

In aqueous colloidal processing of ceramics, the nature and amount of dispersant are important to obtain a stable and uniform dispersed system [5,6]. Well, dispersed slurry with easy followability is achieved by an optimum concentration of the dispersant. Therefore, many physical and chemical processes occur at different interfaces [7,8].

The physical-chemical surface character has been described as a determinant factor in adsorbing polyelectrolytes onto oxide surfaces. Since composed of hydroxyl groups, the acidity or basicity induced by the bulk lattice in such groups seems to be of great relevance in the adsorption process. Thus, many polymers have been investigated as dispersants for ceramic powders but they are mainly synthetic [2]. Naturally occurring polymers are non-toxic and biodegradable and, therefore, do not present problems of handling and disposal that may be encountered with some of their synthetic counterparts [9,10]. Pellerin *et al.* used some acidic biopolymers to serve as dispersants for colloidal processing of ceramics. One biopolymer they tested was alginate, a heteropolysaccharide containing two carboxylic sugar acids, and they found that alginate was a suitable dispersant, provided that its viscosity was reduced by partial acid hydrolysis [11]. The influence of such properties in the adsorption of polyacrylic acid derivative polymers and a basic polymer (Chitosan; CS) onto SnO<sub>2</sub> and Al<sub>2</sub>O<sub>3</sub> surfaces is reported in the literature [12]. Polyacrylate acid molecules are observed to hardly adsorb onto the SnO<sub>2</sub> surface but strongly adsorb, as reported previously, onto the alumina surface. This behavior is explained based on the pronounced difference concerning the acidity of both surfaces.

Herein, we describe the preparation of some novel dispersants based on extracted chitosan and its graft copolymerization of different aliphatic dicarboxylic acids and study their dispersibility and evaluate their type of adsorption isotherms.

## **Experimental**

### *Material*

Shrimp shells were collected from the local market. Dicarboxylic acid with 99% purity was purchased from different sources, Succinic acid (RDH), Glutaric acid, Pimelic acid (Aldrich), Sebacic acid (BDH). All solvents were purchased from Aldrich as well and used as received without any further treatment. Alumina type Reynolds

with 99.9% purity was obtained from MIT with a particle size of around 0.3  $\mu\text{m}$ .

### *Methods*

#### *Collecting Shrimp Shells*

Dry shrimp shells were collected from the local market. They were washed with water many times and then left to dry again under sunlight. Then, it was ground by an electrical mill to be used for the extraction of chitin.

#### *Extraction of Chitin*

One hundred and fifty grams of shrimp shells powders were dried at 100°C for 10 hours in a drying oven, and then 1500 ml of 4% hydrochloric acid solution was added gradually to the powder and stirred mechanically for 24 hours at ambient temperature to remove minerals and their salts. The residual powder was filtered and washed several times with distilled water to remove the residual hydrochloric acid. Then, 1500 ml of 10% sodium hydroxide solution was added to the powder and stirred mechanically for 16 hours at 90°C to remove all protein. The mixture was cooled down to ambient temperature, filtered and washed several times with distilled water to remove residual sodium hydroxide, and dried at room temperature to obtain chitin powders [13,14].

#### *Modification of Chitin to Chitosan*

The deacetylation procedure was used to convert the extracted chitin to chitosan aiming to get a better degree of deacetylation and hence good solubility of chitosan. 30 g of dry chitin was mixed with 350 ml of 60% sodium hydroxide solution and charged in three-neck round bottom flask fitted with a condenser, mechanical stirrer, and thermometer. The mixture was heated up and kept the temperature between 90-100 °C for 12 hours, and then left it to cool down at ambient temperature [15]. Afterward, the sample was filtered and washed continuously with 50 ml of (50%) NaOH and washed several times with distilled water to retain the chitosan. The sample was left to dry in the vacuum desiccator to dry. The white powder product of (CS) was obtained. Scheme (1) illustrates the deacetylation process of chitin.

#### *Purification of Chitosan*

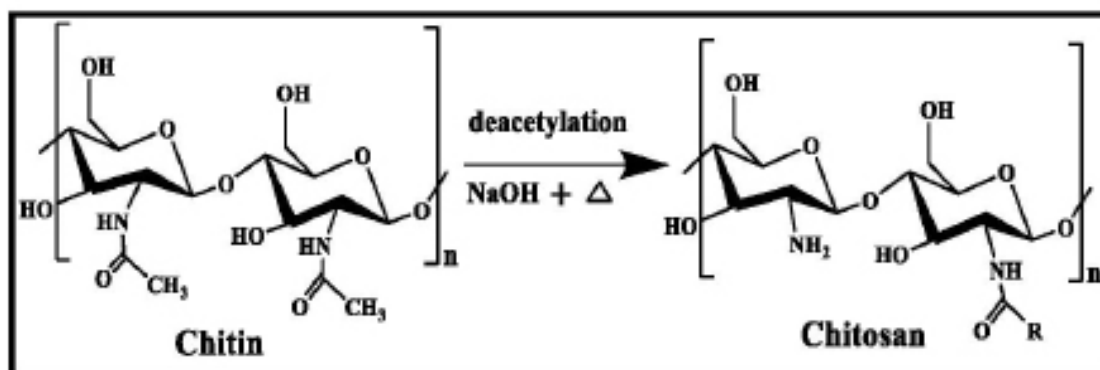
Ten grams of chitosan was dissolved in 100 ml of 2% acetic acid and stirred until a homogenous solution was obtained and stirred mechanically for 24 hours at room temperature, and then the insoluble material was removed by filtration. 4N

NaOH was added gradually to streaming chitosan until a pH value of 8.5 was reached and chitosan precipitates in a viscous form in the solution [16]. The white chitosan powder obtained was washed several times with distilled water, and then filtered and dried.

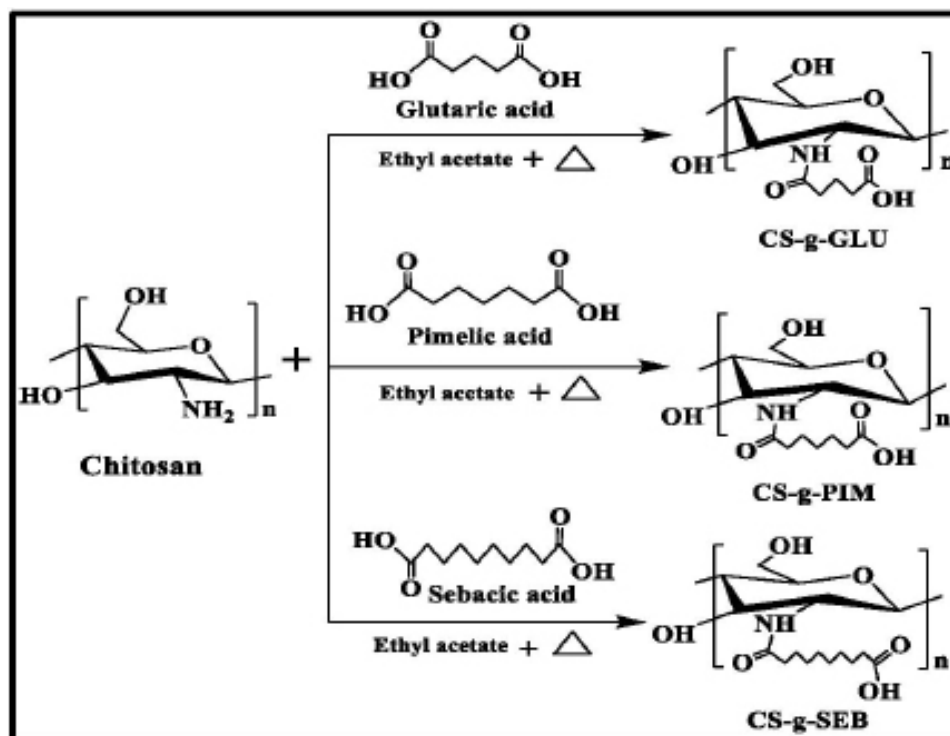
*Preparation of chitosan-grafted-Glutaric acid (CS-g-GLU), Pimelic acid (CS-g-PIM) and Sebacic acid (CS-g-SEB)*

The grafting of Glutaric acid (GLU), Pimelic acid (PIM), and Sebacic acid (SEB) onto chitosan were carried out by the following procedure

[14,16]. 3 g of each acid dissolved in 100 ml ethyl acetate was added to 3 g of chitosan in three-neck round bottom flask fitted with a condenser, magnetic stirrer, and a thermometer, and then the mixture was heated and magnetically stirred at a refluxed temperature of ethyl acetate solvent for 2 hours, and then they left stirring to cool down to ambient temperature. The grafted chitosan with different acids was filtered and washed with ethyl acetate and acetone several times, respectively, and then the white powder products were dried in the vacuum desiccator. Schemes (2) shows the grafting processes.



Scheme 1. Deacetylation reaction of chitin to chitosan.



Scheme 2. Chemical grafting reaction of the chitosan with different dicarboxylic acids.

### Assessment of the Prepared Dispersants

#### Rheological method

The ability of the extracted chitosan and its three dicarboxylic derivatives, i.e. CS-g-GLU, CS-g-PIM, and CS-g-SEB were examined as natural dispersants for alumina particles in 2% acetic acid-water solution. This was done firstly by rheological assessment using a FungiLab Rotational Viscometers Alpha series/Spain.

The concentrations (0.5 %, 1%, 2%, and 3%) of chitosan and chitosan-grafted different dicarboxylic acids were prepared by dissolving the required amount with 30 ml of 2% acetic acid. Then 22.5g of alumina powder was added to 60 ml cylindrical container made especially for this test. The alumina slurry was shaken ultrasonically for 30 minutes to break down any alumina agglomeration may, it is present and to increase the adsorption surface area. Sonication is the phenomenon when ultrasonic waves pass through different folds of sediment disturbing particles. Hence the big agglomerates are broken into smaller agglomerates [17].

Rheological or dynamic viscosity  $\eta$  was measured using spindle R5-rotor and 100 rpm rotation speed of ambient temperature. Each measurement was repeated four to five times to obtain a constant rate of rheological viscosity for each concentration.

#### Centrifugation settlement

The same above concentrations were used, (i.e. 0.5%, 1%, 2%, and 3%) from chitosan and their three grafted-dicarboxylic acids as dispersing agents for alumina powder. This was prepared by dissolving a certain amount of the prepared polymer in 8 ml of 2% acetic acid, and then it's added to the 6 g of alumina powder weighted in a dry centrifuge tube. They were agitated manually for 15 minutes at ambient temperature to increase the surface area of adsorbent and preventing particle accumulation, and then ultrasonically for at least 30 minutes to produce a maximum surface area for the expected adsorption. Then, the dispersed particles were settled down by centrifugal forces at 3500 RPM. The clear supernatant solution above the compact particle layer was removed carefully by decantation. The test tubes were weighed in a sensitive balance before drying. Then dried in the oven at 90 °C, and then weighed until getting a constant weight. The results were expressed by % packing density [2,18].

*Egypt.J.Chem.* **63**, No. 7 (2020)

## Results and Discussion

### Degree of deacetylation (DD) and Molecular weight of Chitosan

The degree of deacetylation is one of the main parameters that characterize chitosan. It was calculated by the absorbance baseline method using infrared spectroscopy [19]. In this procedure, the calculation of DD depends on the absorbance ratio of the two bands at 1630  $\text{cm}^{-1}$  and 3423  $\text{cm}^{-1}$  assigned to amide and the amine absorbance respectively, **Fig. 1**. Degree of deacetylation (DD) was calculated from equation 1 [20], and it is found equal to 93:

$$DD = \frac{1.33 - A_{1630}/A_{3423}}{1.33} \times 100 \quad \dots \dots (1)$$

The molecular weight of chitosan is measured by the viscosity method. It is known that the intrinsic viscosity  $[\eta]$  as a function of viscosity average molecular weight  $M_v$  is represented by the Mark-Houwink-Sakurada equation [21]:

$$[\eta] = kM_v^\alpha \quad \dots \dots (2)$$

Where  $k$  and  $\alpha$ , are constants and their values depend on the type of polymer, solvent, and temperature. Under working conditions,  $k = 9.66 \times 10^{-5} \text{ dm}^3\text{g}^{-1}$  and  $\alpha = 0.742$  [22].

The calculated chitosan viscosity average molecular weight from the Mark-Houwink-Sakurada equation is equal to  $7.4 \times 10^5$  g/mole. However, this value is considered as a moderate value comparing to the lower value of  $3.9 \times 10^5$  g/mole obtained by Yacob et al. [22], and the higher value of  $10.5 \times 10^5$  g/mole obtained by Hossain and Iqbal [23].

### FTIR Characterization

#### The Infrared spectrum of chitosan

Chitosan, in this work, is used as a base material to prepare different polymeric derivatives. FTIR spectrum of pure chitosan is shown in **Fig. 2**. It exhibits broadband with a peak at 3418  $\text{cm}^{-1}$  due to (-OH) stretching and a (-NH) stretching. The aliphatic C-H stretching band appeared at 2924  $\text{cm}^{-1}$  and 2877  $\text{cm}^{-1}$ . A weak band with a peak at 1647  $\text{cm}^{-1}$  assigned for amide I which was left from the deacetylation process, verified that chitosan with a high degree of deacetylation was obtained. Also, the appearance of a strong band at 1420  $\text{cm}^{-1}$  due to (C-N) stretching bond confirms the

deacetylation process [14,18]. The band at  $1574\text{ cm}^{-1}$  corresponds to the N-H bending vibration of the amino group. The absorption bands at

$1150\text{ cm}^{-1}$  assigned for (-C-O-C) glycosidic linkage, and at  $1064\text{ cm}^{-1}$  (C-C stretching) are characteristics of the polysaccharide structure.

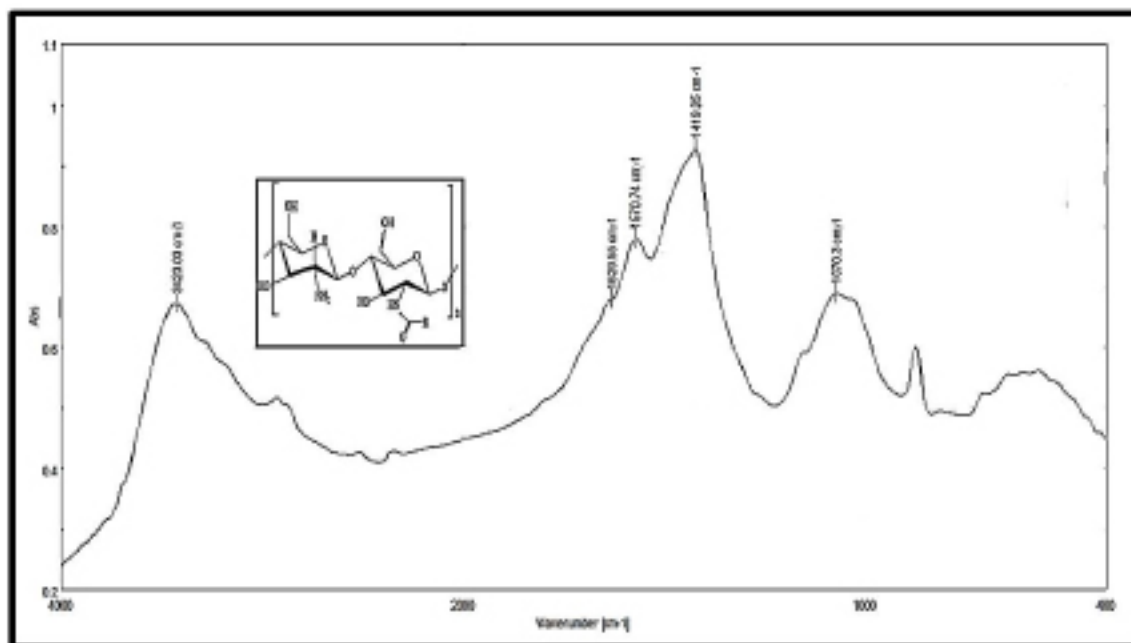


Fig. 1. FTIR of chitosan in absorbance mode used for estimation the degree of deacetylation.

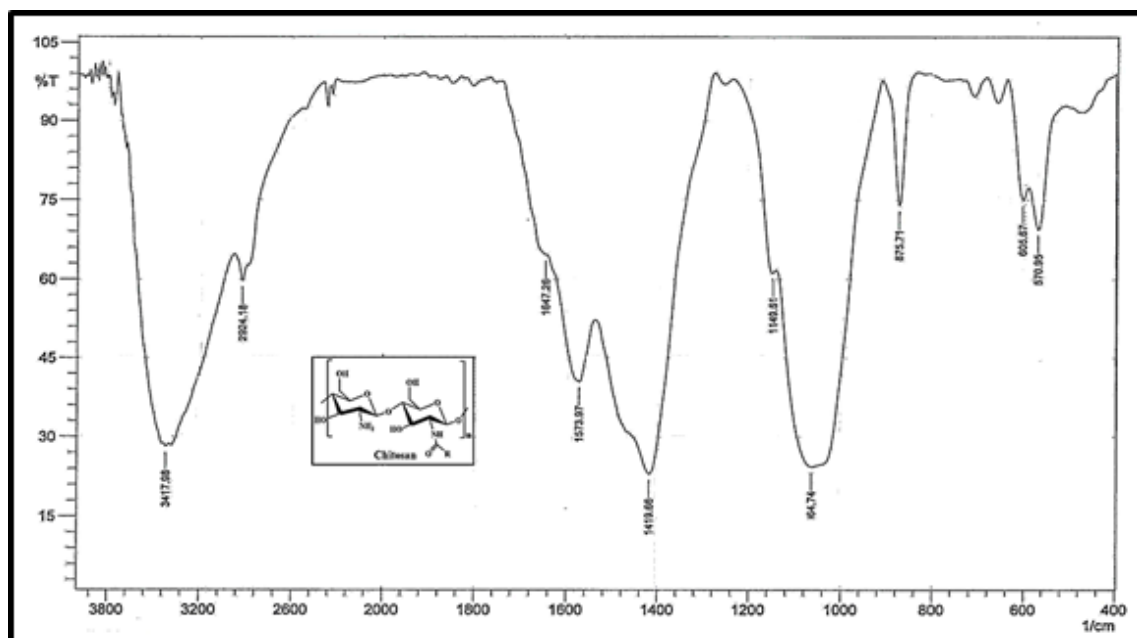


Fig. 2. FIR spectrum of chitosan.

### Characterization of Chitosan-g-acid derivatives by FTIR

Synthesis of functionalized chitosan by grafting allows more applications for the natural polymeric chitosan. Chitosan has strong reactive basic amino groups that can be used as grafting centers of different compound and polymer onto the chitosan backbone [24], to suit our target applications, and this is the case here. The most characteristic region that has to be examined of

the chitosan-g-acid derivatives spectra is the C=O stretching region. Their spectra are clearly shown the presence of the carbonyl group stretching depending on the type of the grafted acid and they appear as follow: grafted glutaric acid at  $1697\text{ cm}^{-1}$ , grafted pimelic acid at  $1724\text{ cm}^{-1}$ , and at  $1701\text{ cm}^{-1}$  for grafted sebacic acid, and their FTIR spectra are shown in **Figs. 3, 4, and 5**. These results imply that real grafting was obtained.

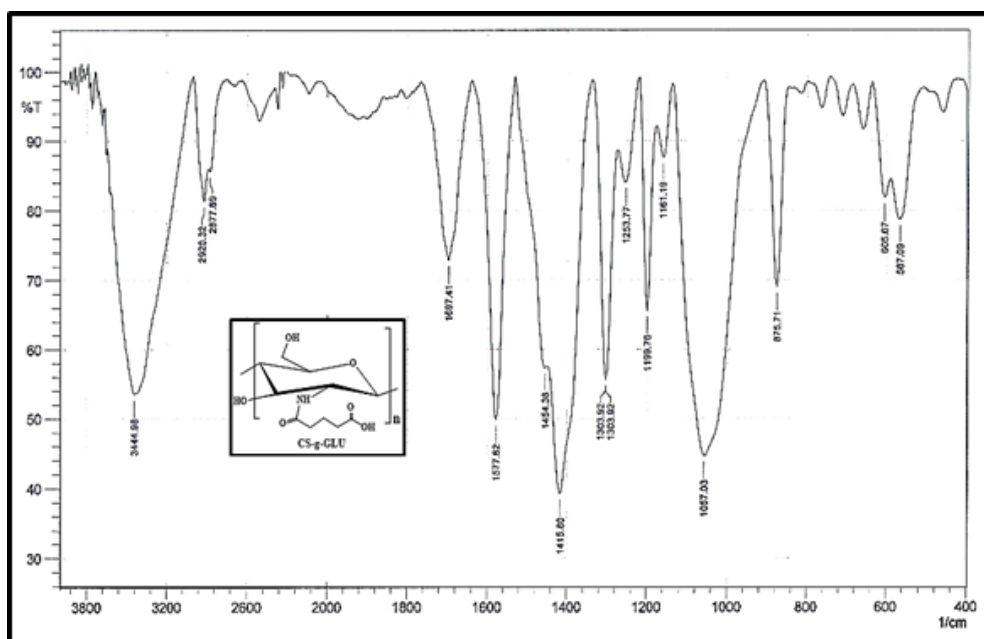


Fig. 3. FTIR spectrum of CS-g-GLU.

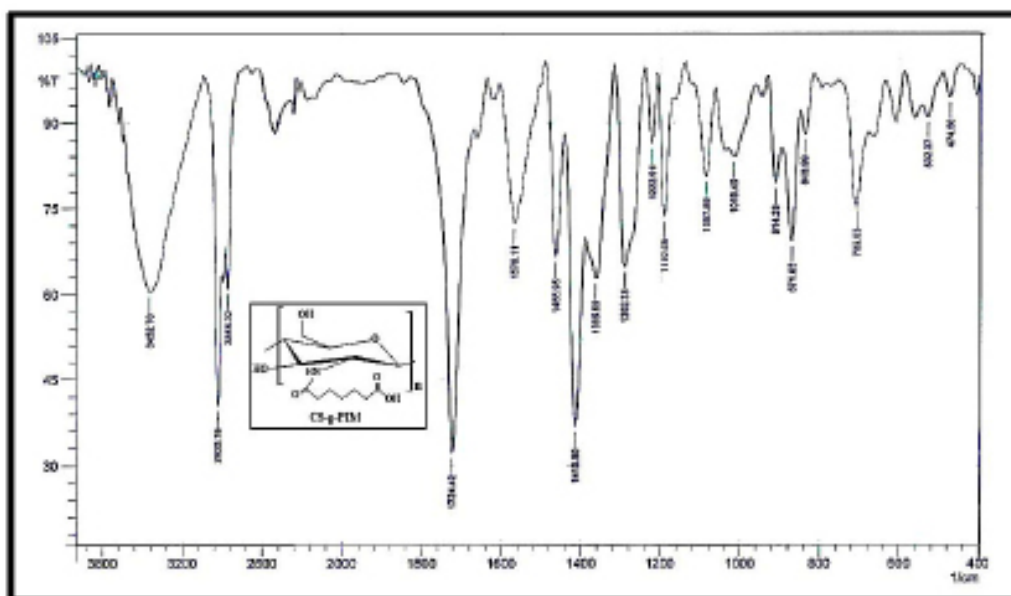


Fig.4. FTIR spectrum of CS-g-PIM.

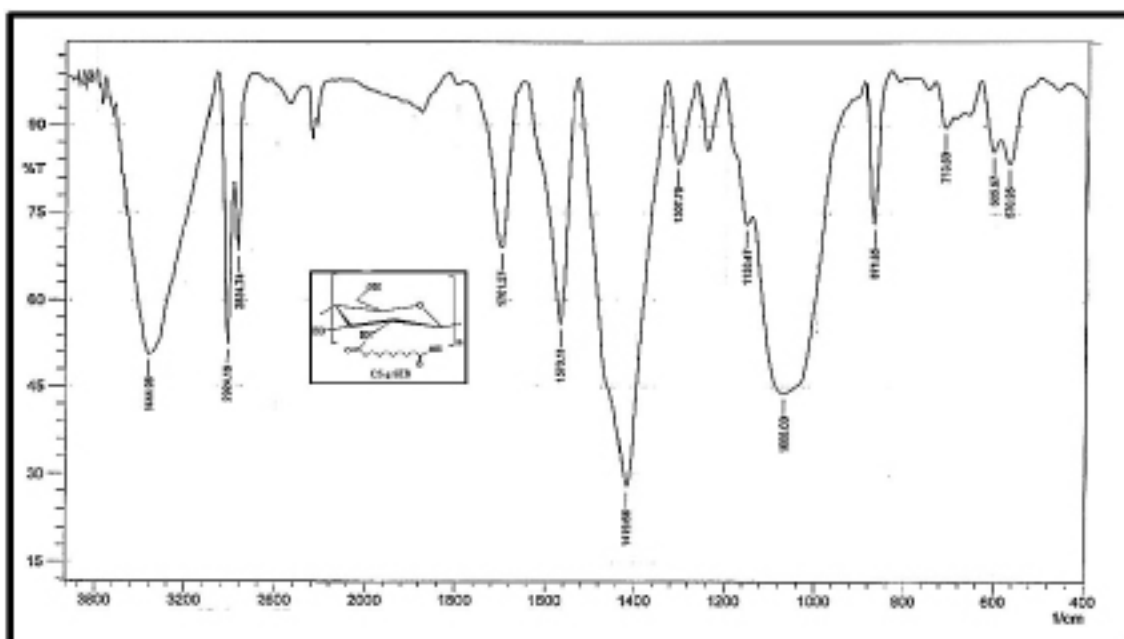


Fig. 5. FTIR spectrum of CS-g-SEB.

#### *Effect of different dispersants on the dispersion of alumina*

Alumina powder is chosen as a model due to its wide applications in advanced ceramics, and to study the effects of differently prepared dispersants on the rheological and packing density of its suspensions. Fine particles of alumina powder, due to their large surface area, often tend to form agglomerates during processing and result in suspensions with high viscosity and poor packing behavior. It is thus generally accepted that the successful application of this technique to fine particles depends to a great deal upon the choice of dispersant [25].

#### *Rheological behavior of alumina suspensions*

Since the physical measurements of any dispersion can lead to a better understanding of the state of dispersion, rheological test, measured in terms of viscosity, was performed first using different concentrations of chitosan and its acidic derivatives as described above. The measurement results of  $\eta$  are shown in Fig. 6.

These results showed that using alumina with 2% acetic acid as a dispersion medium only produced alumina slurry with a high viscosity. Meanwhile, it is quite obvious that the addition of all dispersants enhances the viscosity of alumina

suspension, especially at lowest two wt.% concentrations of all dispersants used (i.e. 0.5 and 1%), and then the suspension viscosity started to increase with increasing the concentration of the dispersants added up to 2wt% and then leveling off to plateau region with slight difference in the case of CS-g-SEB. This behavior may give the impression that maximum adsorption occurred on the alumina surface, and the viscosity is affected by the quantity of un-adsorbed dispersant. From these preliminary measurements, we can conclude that the prepared grafted acidic chitosan and chitosan itself have a positive effect on the dispersibility of alumina particles in acetic acid solution as a dispersion medium.

The adsorbed chitosan grafted acids onto alumina was also examined by FTIR, Fig. 7. It shows clearly the disappearance of the peak assigned for acidic carbonyl groups from the region  $1700\text{ cm}^{-1}$  due to the adsorption process and appears in the form of a new band having a maximum at  $1550\text{ cm}^{-1}$ , Fig. 7, which was visible in all interface spectra of alumina/chitosan-g-acids derivatives. These bands are assigned to the stretching vibration of carboxylates resulting from the adsorption of acid derivatives onto basic alumina surface [3,8]. This implies that the grafted chitosan with different acids led to enhance the

polymer adsorption onto alumina powder, as a result of the acid-base interaction between the

acidic carboxyl groups and the basic alumina surface sites, as shown schematically in Fig. 8.

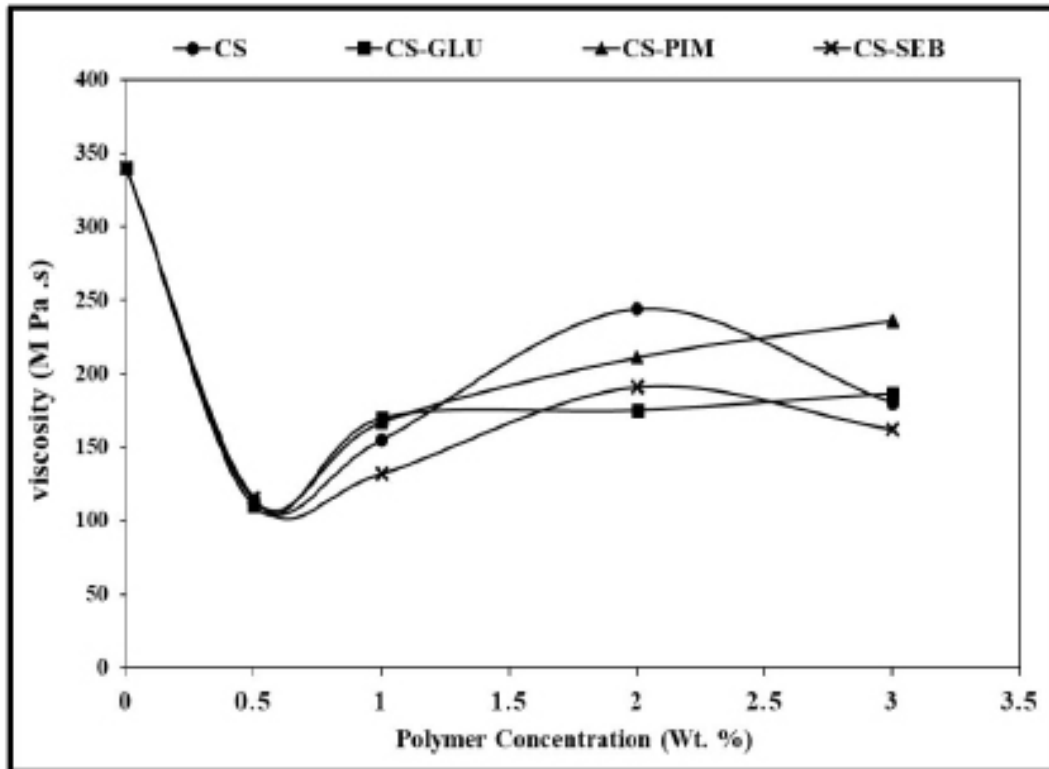


Fig. 6. Effect of wt% of chitosan and its acidic derivatives on the viscosity of the alumina dispersions using CS, CS-g-GLU, CS-g-PIM, and CS-g-SEB as dispersants.

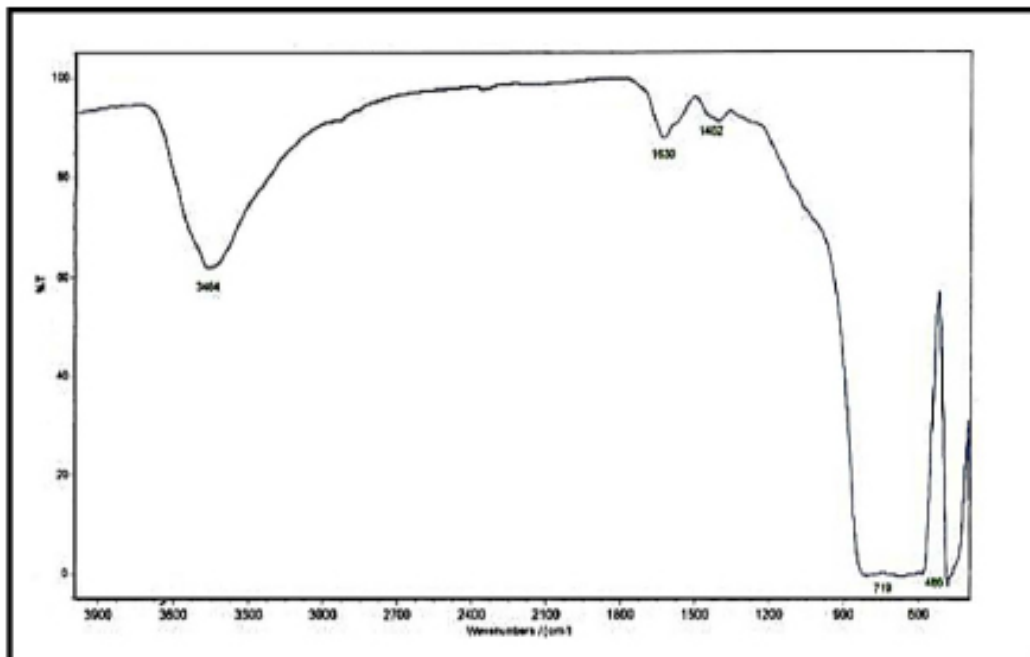


Fig. 7. The extracted DRIFT spectrum of the adsorbed acid onto alumina surface from alumina itself.



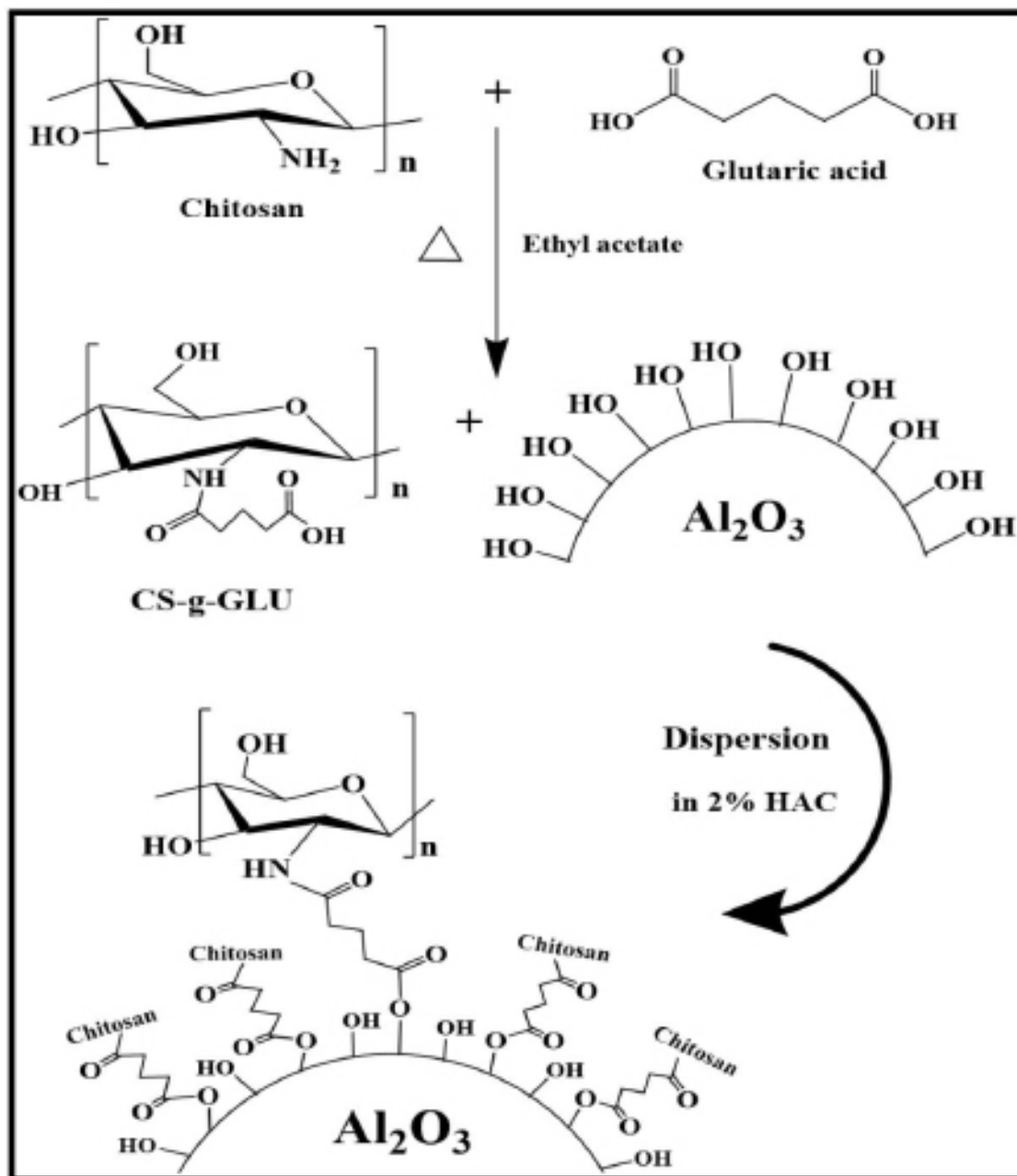


Fig. 8. Schematic representation of chitosan-grafted-acid dispersant adsorbed onto alumina surface.

#### *Qualitative observations of Dispersion Stability*

The extent to which the individual powder particles become separated from one another in their dispersed liquid medium is defined as a degree of particle dispersion [26]. Measuring the final packing density of the alumina beds and monitoring the rate of settled alumina particles from their dispersion medium are considered as the common methods to evaluate the ability of the chitosan and its prepared grafted acid polymers to act as dispersalagents for alumina particles; slow

settling and/or better packing density are taken as an indication for good dispersion stability. In this work, the settling behaviors of chitosan and chitosan-g-acid derivatives are compared to each other and with that of alumina/acetic acid solution suspension only.

Alumina particles were settled under gravity using 1 wt. % of CS, CS-g-GLU, CS-g-PIM, and CS-g-SEB as dispersants dissolved in 2% acetic acid solution as a dispersing

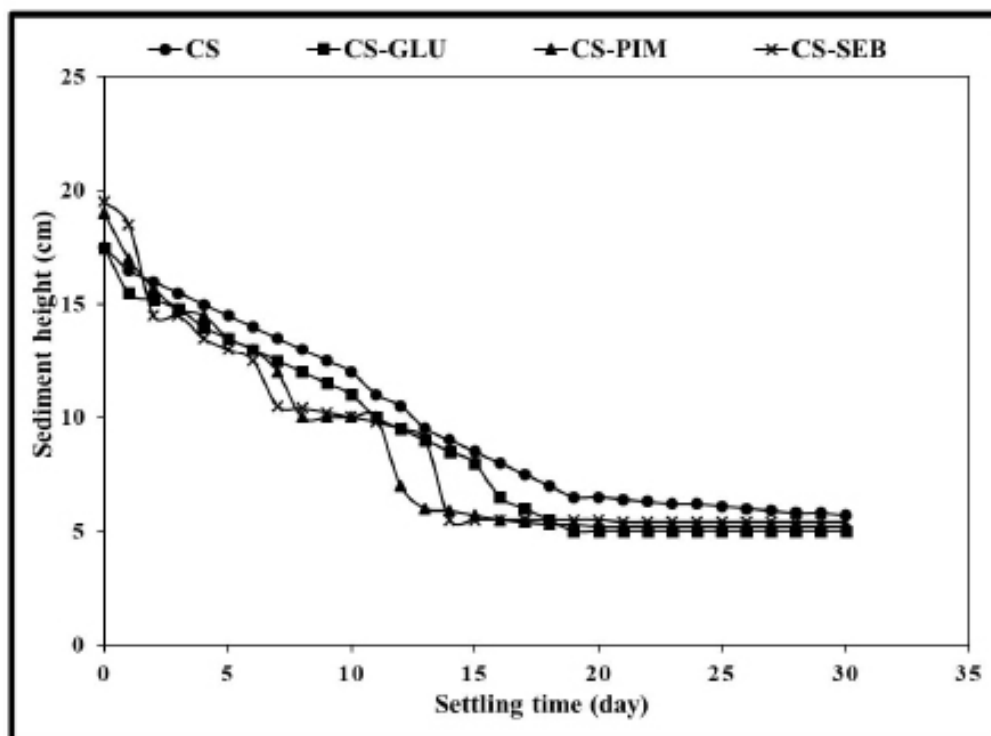


Fig. 9. Height of alumina sediments as a function of settling time using CS, CS-g-GLU, CS-g-PIM, and CS-g-SEB as dispersants.

medium as described. The speed at which the interface between the supernatant liquid and the combining sediment moved down represents the sedimentation rate of the settling. This gives us a chance to compare these different dispersions in terms of settling rate and final sediment volumes directly. Although all the polymers used as dispersants contributed to the dispersibility of alumina into the acetic acid solution, some of them increased the stability of the dispersions very much more than others, as shown in Fig. 6, which compares the top particle height versus settling time for all the dispersants used. In the case of alumina suspension with no dispersant added, it was difficult to measure the sediment height and hence the settling rate due to that most of alumina particles adhered strongly to the inside wall of the cylinder, and this agreed very well with results reported in the literature [2,18].

The final sediment height of the compact beds is of different values, as seen in Fig. 9, and all the grafted acid chitosan's were lower than that of chitosan itself, implying very much better packing of particles. This type of sedimentation behavior is typical of deflocculated dispersions [27], and alumina dispersion settled in CS-g-GLU had a slower settling rate and lowest alumina bed

volume.

#### *Effect of dispersants on the packing density*

The packing density of the final particle bed was measured and is expressed as a fraction of the theoretical density of fully dense alumina particles. The perfect packing of spheres would yield a density of 74%; random close packing of spheres gives 69% density. Agglomerated particles typically settle rapidly to packing densities of the order of 20%. Dispersants giving packing densities in the range from 30% to 60% are currently regarded as good dispersants [3,18].

During the preparation of the testing adsorption experiment samples for determination of packing density by centrifugation, it was noticed that alumina powder in 2% acetic acid was coagulated and most of the powder adhered to the inside wall of the tube. This observation disappeared when the chitosan and chitosan grafted acid solution with 2% acetic acid was added to the alumina. This implies that the addition of the dispersants considerably enhanced the dispersibility of the alumina in acetic acid solution, and hence the degree of deflocculating. The effect of dispersant concentrations on the dispersion of alumina particles was measured after centrifugation settlement as described before. The results

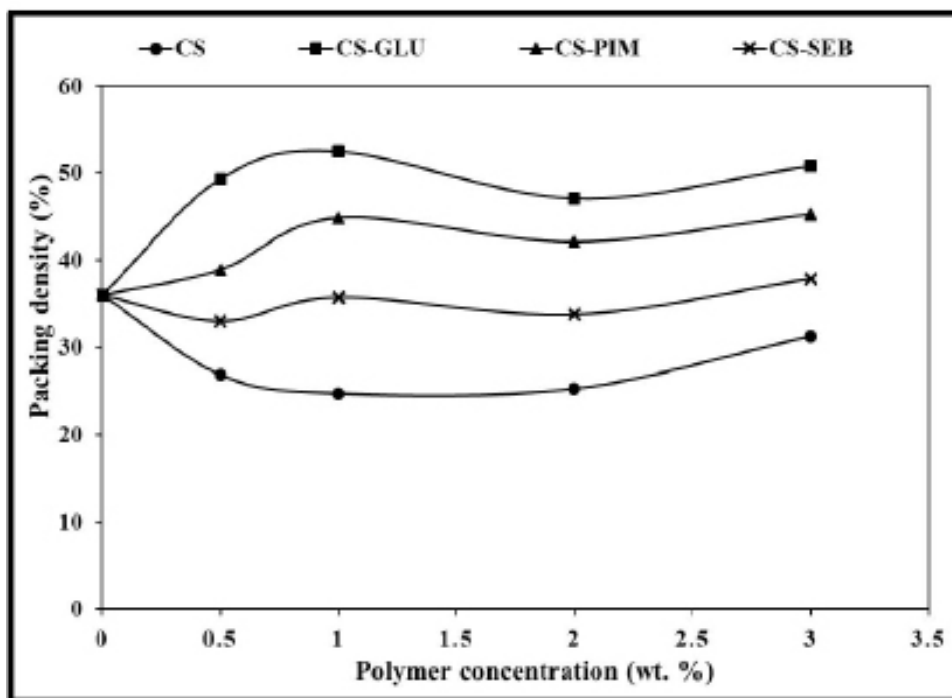


Fig. 10. Effect of the dispersant concentrations on the packing density of alumina.

obtained are shown in Fig. 10.

The packing densities obtained with chitosan-grafted-acids were much higher than ungrafted chitosan. About 1% polymer concentration was needed to get a maximum packing density for all the grafted chitosan and CS-g-GLU acid being the best. Increasing adsorption is accompanied by a very slight decrease in packing density, in contrast with ungrafted chitosan. Its packing density slightly increases with increasing the adsorption process, giving the impression that physisorption may take place in the case of chitosan [28].

#### Adsorption isotherms

A layer of a polymer can be formed on the surface of the alumina in the adsorption process. It is usually described in terms of adsorption isotherms and is defined as the amount of polymer on the alumina as a function of its concentration at a constant temperature. This relates the amount of polymer adsorbed at the alumina particle  $q_e$  (mg/g) with the amount of polymer in solution  $C_e$  (mg/L). The amount adsorbed is nearly always controlled by the mass of the adsorbent to make a comparison between different materials easy and possible. Adsorption isotherm can be defined as the study of the relation between the amounts of adsorbed dispersant on the surface of alumina at a constant temperature.

Adsorption reduces the disparity of attractive forces that happens at the surface leading to the formation of the surface free energy of a heterogeneous system [29]. In the present study, the quantity of adsorbed dispersants was determined by thermal gravimetric analysis, and hence the equilibrium isotherms are measured to determine the capacity alumina powder for chitosan and its acid-grafted derivative dispersants. Our experimental results were fitted for four isotherm equations and they are; Langmuir isotherm, Freundlich isotherm, BET isotherm, and Dubinin–Radushkevich isotherm. The isotherm analyses based on the constants obtained from the linearized plots and correlation coefficient  $R^2$  from the equations reported for each isotherm are discussed. Before we move further to determine which isotherm(s) is more suitable for our data results.

The amount of adsorbed dispersant per unit weight of the alumina ( $q_e$  in mg/g) estimated by thermal gravimetric analysis [35] was plotted versus the equilibrium concentration of the dispersant left in the solution ( $C_e$  in mg/L). The plot of  $q_e$  versus  $C_e$  is shown in Fig. 11.

#### Langmuir isotherm

The nonlinear representations of Langmuir isotherm are given by equations 3 and 4 [31,32]:

$$q_e = \frac{q_{max}K_L C_e}{1 + K_L C_e} \quad \dots \dots \dots (3)$$

$$q_e = q_e K_L \frac{C_e}{1 + K_L C_e} \quad \dots \dots \dots (4)$$

The adsorption equilibrium experimental points were investigated firstly to show whether they fit or not with the Langmuir isotherm, and it is necessary to examine the shape of Langmuir adsorption isotherm curves obtained, which appears nearly close to S-type as classified

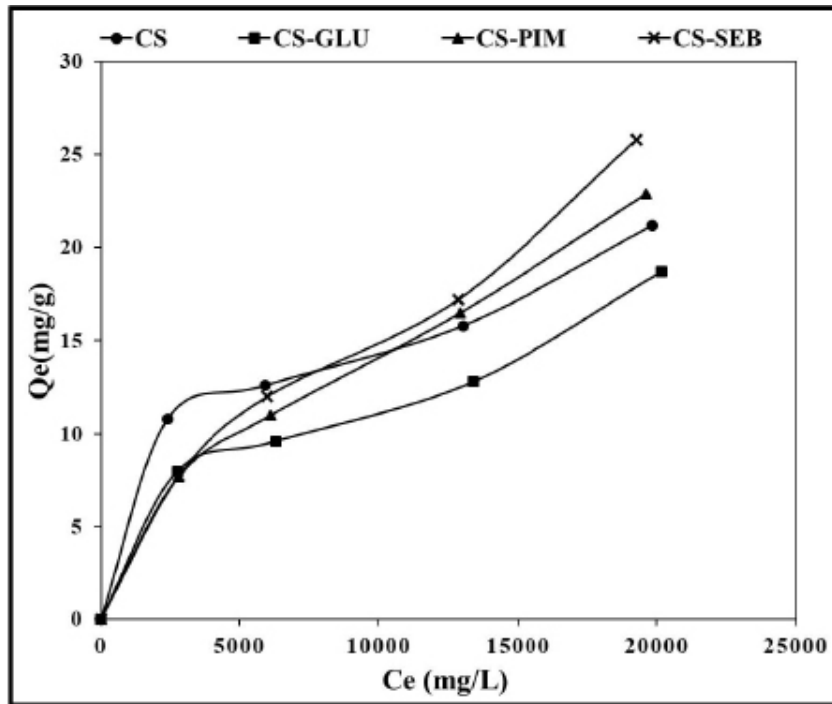


Fig. 11. Equilibrium adsorption of chitosan and its grafted acid derivatives, CS, CS-g-GLU, CS-g-PIM, and CS-g-SEB.

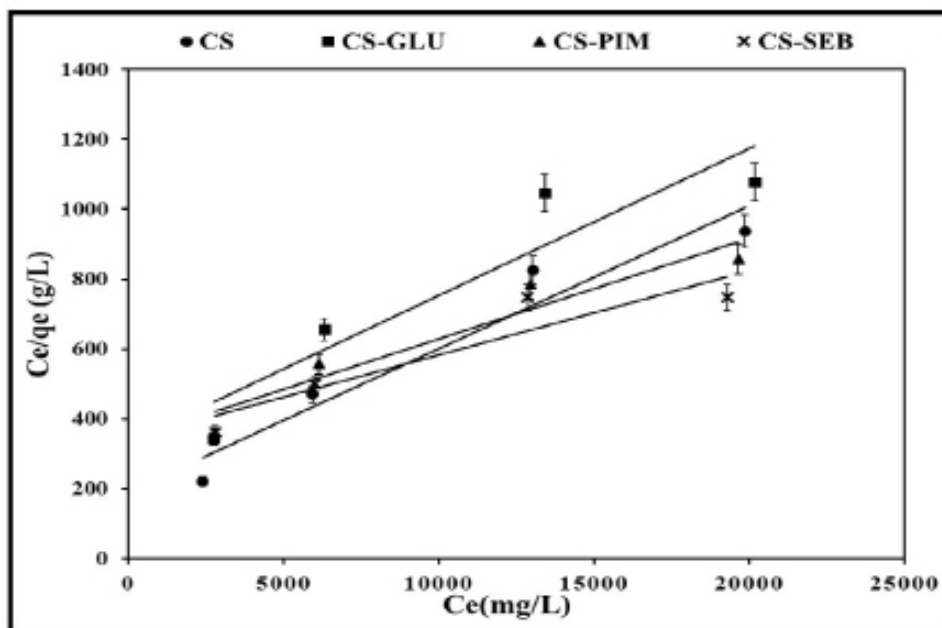


Fig. 12. The Langmuir isotherm plot of adsorption of all dispersant onto alumina particles using equation 6.

by Gilles et al. refereeing to a monolayer coverage [32].

The influence of the adsorption isotherm shape can be examined whether adsorption is favorable in terms of  $R_L$ , a dimensionless constant referred to as equilibrium parameter.  $R_L$  is related to the  $K_L$ , the Langmuir constant (L/mg) and related to the energy of adsorption, and  $C_i$ , the dispersants initial concentration, by the following relationship represented by equation 5 [36, 37]:

$$R_L = \frac{1}{(1 + C_i K_L)} \quad \dots \dots (5)$$

Langmuir isotherm can be represented by the linearized two following forms [34,35]:

$$\frac{C_e}{q_e} = \frac{1}{q_{\max} \cdot K_L} + \frac{C_e}{q_{\max}} \quad \dots \dots (6)$$

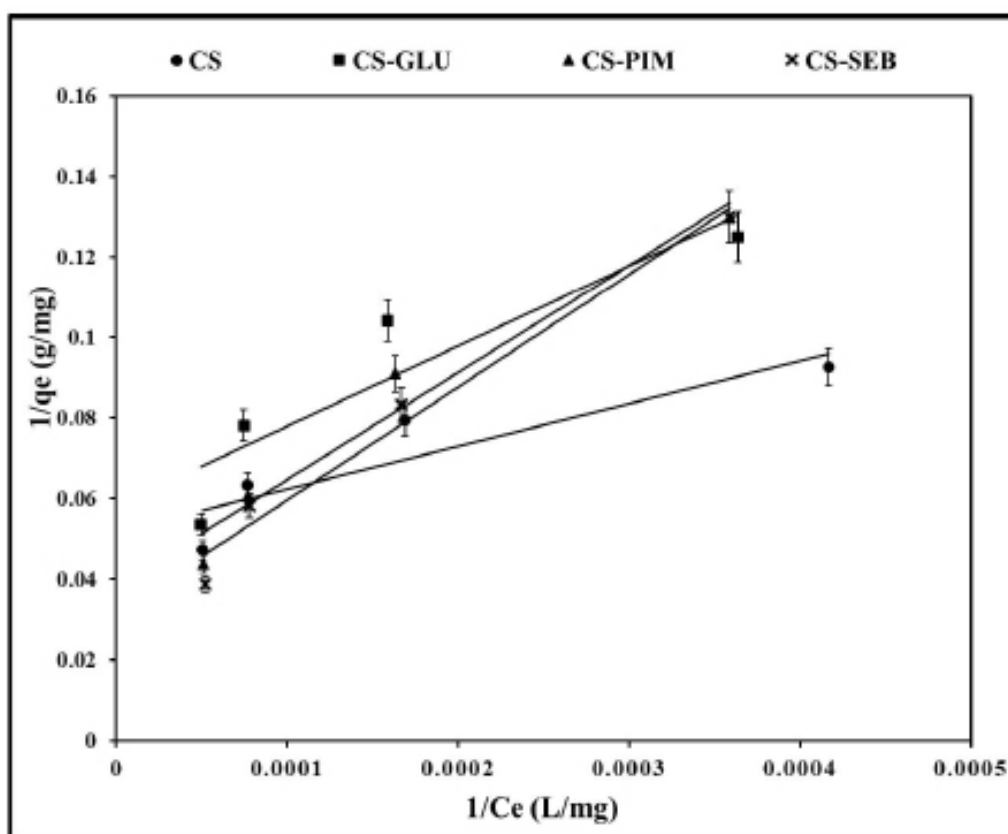


Fig. 13. The Langmuir isotherm plot of adsorption of all dispersant onto alumina particles using equation 7.

TABLE 1. Constant parameters and correlation coefficients calculated for Langmuir adsorption isotherm equations.

Type of Dispersant	Langmuir equation (6)				Langmuir equation (7)			
	$q_{\max}$ (mg/g)	$K_L$ (L/mg)	$R_L$	$R^2$	$q_{\max}$ (mg/g)	$K_L$ (L/mg)	$R_L$	$R^2$
CS-ALO	24.450	0.00021	0.3376	0.9367	19.380	0.00048	0.1939	0.8146
CS-GLU-ALO	23.753	0.00013	0.4489	0.8701	17.271	0.00029	0.2783	0.8358
CS-PIM-ALO	34.602	0.00009	0.5385	0.9183	26.316	0.00014	0.4225	0.9607
CS-SEB-ALO	41.494	0.00007	0.5796	0.8626	31.546	0.00011	0.4739	0.9770

$$\frac{1}{q_e} = \frac{1}{q_{\max}} + \frac{1}{K_L q_{\max}} \frac{1}{C_e} \quad \dots \dots \dots (7)$$

Where :  $q_{\max}$  is the maximum adsorption (mg/g). These values can be obtained from the linear form of equations 6 and 7. The results obtained are shown in Fig. 12 for equation 6 and Fig. 13 for equation 7, and  $q_{\max}$  calculated from the intercept,  $K_L$  calculated from the slope, are all listed in Table 1 with the correlation coefficient  $R^2$ .

The elemental characteristic of the Langmuir adsorption isotherm gives a valuable indication that whether adsorption is favorable in terms of the dimensionless constant  $R_L$ . Favorable

adsorption required is  $0 < R_L < 1$ , while  $R_L \geq 1$  means unfavorable or linear isotherm respectively, and when  $R_L = 0$ , this is a sign for the irreversible adsorption. It is obvious from Table 1, all  $R_L$  values lie between 0 and 1 revealing that favorable adsorption of chitosan and chitosan derivatives dispersants onto alumina surface took place. It looks like chitosan has the lowest values implying that it is nearly unfavorable adsorption may occur, which is the case here, and this conclusion agreed very well with the measurements of rheology, settling rate, and packing density as discussed above.

Assessment of the  $q_{\max}$  values listed in Table 1 indicated that the  $q_{\max}$  of adsorbed chitosan-

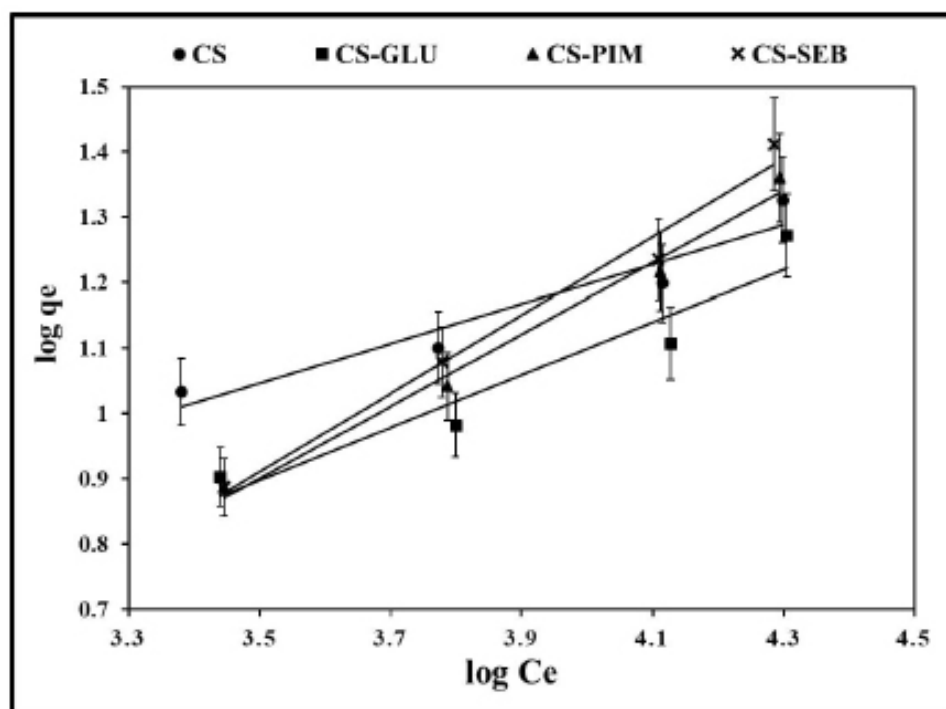


Fig. 14. The Freundlich isotherm plot of chitosan and its different acid derivatives onto alumina.

TABLE 2. Parameters for plotting Freundlich adsorption isotherms of different dispersants onto alumina.

Type of Dispersant	Freundlich Parameters		
	$K_f$ (mg/g)	$n$	$R^2$
CS-ALO	0.9779	3.3134	0.9182
CS-GLU-ALO	0.3055	2.4777	0.9156
CS-PIM-ALO	0.0957	1.8218	0.9885
CS-SEB-ALO	0.0662	1.6739	0.9826

grafted glutaric acid had the lowest value, and it may be explained in term of coverage, whereas chitosan-grafted pimelic acid and sebacic acid had the higher  $q_{max}$ , even with ungrafted chitosan, and this clearly seen in Fig. 11 and with rheological measurement results shown in Fig. 6.

#### Freundlich isotherm

The Freundlich isotherm is based on the earliest known model describing the non-ideal and reversible adsorption. It can be used to express multilayer adsorption on a heterogeneous surface. The nonlinear Freundlich isotherm model is given by equation 8 [8]:

$$q_e = K_f C_e^{\frac{1}{n}} \quad \dots \dots \dots (8)$$

Where  $K_f$  (mg/g) is the constant related to the adsorption capacity and  $n$  is the empirical parameter correlated to the intensity of adsorption, and its value varies according to the heterogeneity of the adsorbent. Favorable adsorption process occurs with value of  $1 < n < 10$  [36]. The values of  $K_f$  and  $1/n$  are determined from the intercept

and slope of the linearized form of the Freundlich isotherm equation 9 respectively :

$$\log q_e = \log K_f + \frac{1}{n} \log C_e \quad \dots \dots \dots (9)$$

The resulted plot of the  $\log q_e$  versus  $C_e$  is shown in Fig. 14 and the calculated constant from the slope and the intercept beside  $R^2$  are listed in Table 2. All  $n$  values obtained from the Freundlich model are greater than 1 for all types of dispersants used; implying that adsorption of chitosan and chitosan-grafted acid onto alumina was favorable as seen from Table 2.

#### Dubinin-Radushkevich isotherm

The D-R adsorption isotherm is used to distinguish between physical and chemical adsorption from the single solute system[37]. It even has a similar approach to Langmuir isotherm by rejecting the homogenous surface or constant adsorption potential; D-R version is more general than the Langmuir version in exploring adsorption isotherm, and it is defined by equation 10[38]:

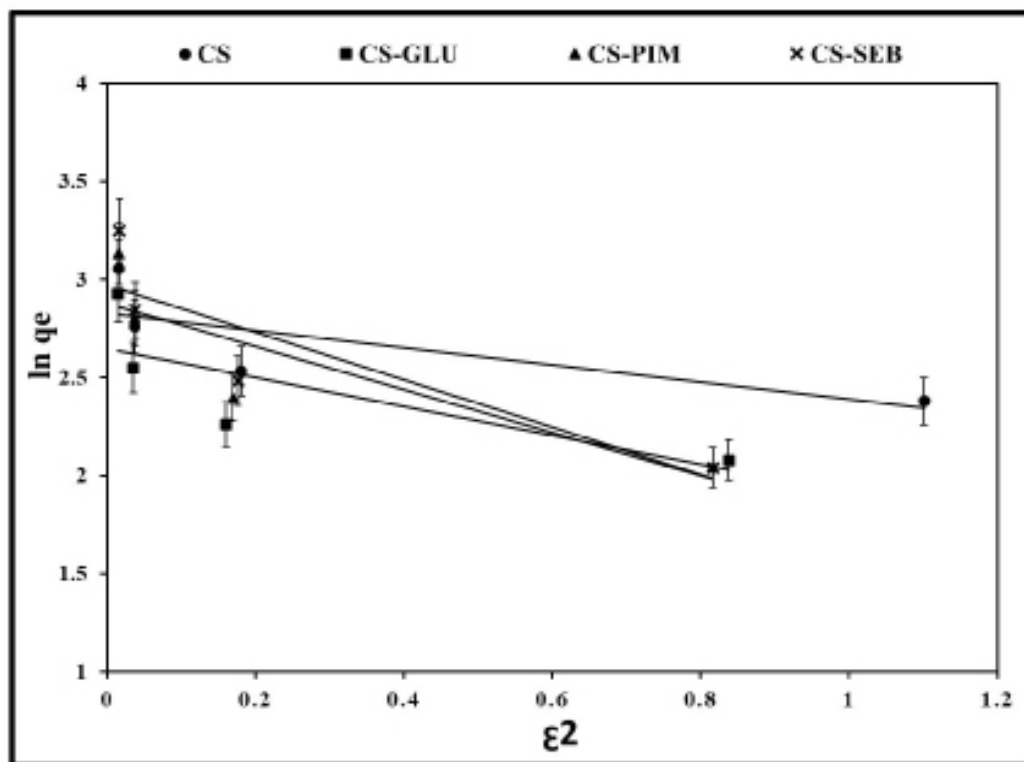


Fig. 15. The Dubinin-Radushkevich isotherm resulted from the adsorption of dispersants used onto alumina particles.

$$q_e = q_{\max} \exp - \beta \varepsilon^2 \quad \dots \dots \dots (10)$$

Where  $q_{\max}$  is the D-R monolayer capacity (mg/g),  $\beta$  is a constant related to adsorption energy ( $\text{mol}^2/\text{kJ}^2$ ), and  $\varepsilon$  is the Polanyi potential which is related to the equilibrium concentration, as shown in the equation 11 [39]:

$$\varepsilon = RT \ln \left( 1 + \frac{1}{C_e} \right) \quad \dots \dots \dots (11)$$

The equation of D-R isotherm model equation 11 can be linearized in the following mode:

$$\ln q_e = \ln q_{\max} - \beta \varepsilon^2 \quad \dots \dots \dots (12)$$

A plot of the amount of adsorbed dispersants in the form of  $\ln q_e$  vs  $\varepsilon^2$  is shown in Fig. 15. The constants such as  $q_{\max}$ ,  $\beta$  were determined from the intercept and the slope respectively. While  $E$  also in a more direct inter way describes the degree of interaction between the adsorbate molecule and the adsorbent surface [40,41]. The calculated results are listed in Table 3.

$$E = \frac{1}{\sqrt{2\beta}} \quad \dots \dots \dots (13)$$

From the linear plot of D-R model,  $q_{\max}$ ,  $\beta$  ( $\text{mol}^2/\text{kJ}^2$ ),  $E$  (kJ/mole) and  $R^2$  are determined and listed in Table 3. The value of was found in

the range of which the mean of  $E$  equal to 0.793 kJ/mol indicating a physisorption process, and the mean of correlation factor was in the rang 0.5952-0.7813, and the means  $R^2 = 0.79$  which were lower than Langmuir and Freundlich isotherms, giving an impression that might not be applicable with the adsorption of the dispersants used, i.e. chitosan and its acid derivatives [42].

#### Brunauer–Emmett–Teller (BET) isotherm

BET model is more general multilayer adsorption in concerned sites randomly covered by a number of dispersed layers. The view of the BET adsorption isotherm is considered as an expansion in the line of the Langmuir theory. It adopts the Langmuir isotherm, which applies to each layer and that no migration happens between different layers. The BET isotherm can be expressed in equation 14 [36]:

$$q_e = \frac{K_B \cdot C_e \cdot q_{\max}}{(C_s - C_e) \{1 + (K_B - 1)(C_e/C_s)\}} \quad \dots \dots \dots (14)$$

BET equation 14 can be rearranged in the following form:

$$\frac{C_e}{(C_s - C_e) \cdot q_e} = \frac{K_B - 1}{K_B \cdot q_{\max}} \times \frac{C_e}{C_s} + \frac{1}{K_B \cdot q_{\max}} \quad \dots (15)$$

Where  $C_s$  is the saturated surface concentration

**TABLE 3. Parameters for plotting D-R adsorption isotherms of different dispersants onto alumina.**

Type of Dispersant	D-R Parameters			
	$q_{\max}$ (mg/g)	$\beta$ ( $\text{mol}^2/\text{kJ}^2$ )	$E$ (kJ/mole)	$R^2$
CS-ALO	16.9116	0.4377	1.069	0.5952
CS-GLU-ALO	14.1244	0.7358	0.825	0.5989
CS-PIM-ALO	17.7805	1.0951	0.676	0.756
CS-SEB-ALO	19.5407	1.2102	0.643	0.7813

**TABLE 4. Parameters for plotting BET adsorption isotherms of different dispersants onto alumina.**

Type of Dispersant	D-R Parameters			
	$C_e$ (mg/g)	$C_s$ (mg/g)	$K_B$ (L/g)	$R^2$
CS-ALO	10300	19850	4.51	0.9785
CS-GLU-ALO	10653	20163	4.71	0.9808
CS-PIM-ALO	10372	19638	10.95	0.9828
CS-SEB-ALO	10228	19275	8.12	0.9740



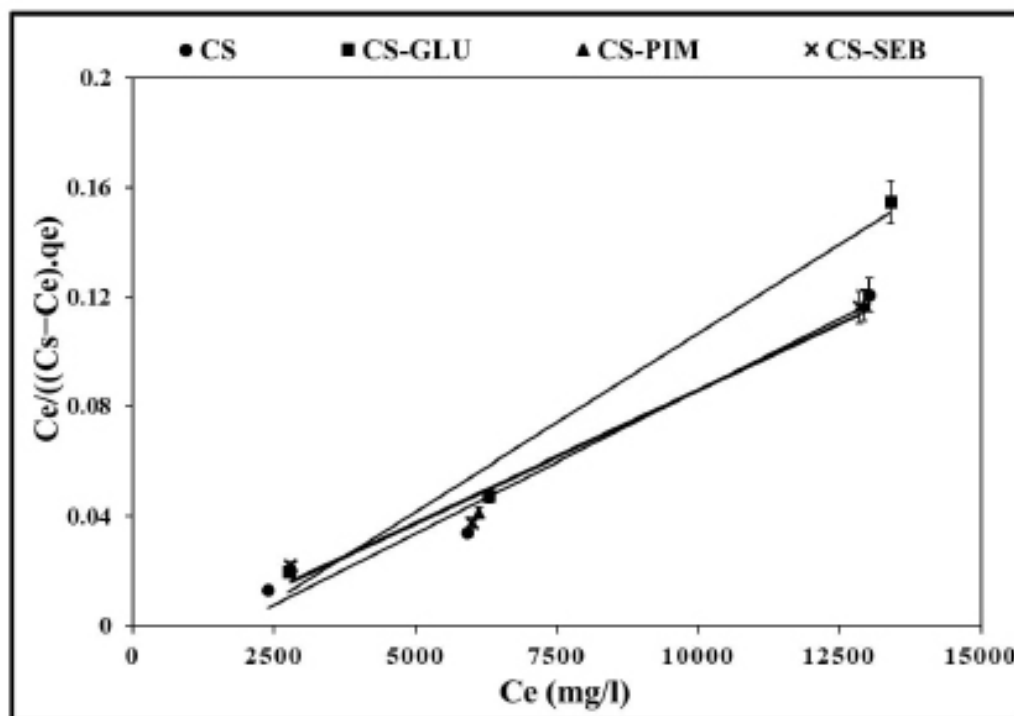


Fig. 16. BET adsorption isotherm resulted from adsorption of chitosan and its acid derivatives onto alumina.

of the dispersant (mg/liter),  $K_B$  is a parameter related to the binding intensity for all layers, and they are calculated from the intercept and slope of the linear lines shown in Fig.16, resulting from plotting

$$\frac{C_e}{(C_s - C_e) \cdot q_e} \text{ vs } C_e$$

The determined BET parameters are listed in Table 4. It is worth to mention here that when  $C_e \ll C_s$  and  $K_B \gg 1$ , BET isotherm approaches Langmuir isotherm as both of them are applicable in case of chemisorption and physisorption [43,44].

A first impression is that the BET equation fitted better the equilibrium data of all dispersants presenting the best correlation ( $0.9785 < R^2 < 0.9828$ ). Freundlich model fitted well for the data with slightly lower correlation coefficients though,  $0.9156 < R^2 < 0.9885$ . Langmuir equation also fitted well for the data, ( $0.8626 < R^2 < 0.9367$ ) obtained with equation 6 and in the range of ( $0.8146 < R^2 < 0.9770$ ) from equation 7. Dubinin-Radushkevich isotherm was not able to reach the level of satisfaction fitting in this study, presenting the lowest correlation of  $0.5952 < R^2$

$< 0.7813$ . So, the adsorption evaluation regarding the adsorption mechanism is in favor of BET and Langmuir-Freundlich isotherms, implying that these three isotherm models can satisfactorily explain the adsorption data. The applicability of the three isotherm models to the adsorption of chitosan-grafted acids onto the alumina surface suggests that both monolayer adsorption and heterogeneous surface conditions are present. The same findings were reported in some of the literature when applied to the experimental data of liquid-phase adsorption [45,47].

### Conclusions

Chitosan as dispersant produces the lowest results for all the properties studied and mentioned so far, although, in counting mostly the higher amount of adsorbed chitosan ( $q_e$ , mg/g). These results gave an impression that chitosan chains may act as bridges between alumina particles, rather than lying flat on the surface of alumina particles. Different behaviors were observed with chitosan-grafted with different acids by increasing the electrostatic repulsions between alumina particles which allow the chitosan-grafted acids chains to be less stretched out, i.e. in a more folded conformation implying that the chains may be

adsorbed more flatly on the surface, considering the experimental fraction of the surface coverage. A similar conclusion was reached by Demarger-André & Domard[47]. This specifies the statement that the acid grafted chitosan chains do not firmly lay flat on the particle surface, and hence the dispersibility increases as the fraction of loops of the adsorbed dispersant increases[48,49].

## References

- Duvarci Ö. Ç., Rheological behavior of nanocrystalline/submicron ceramic powder dispersions, PhD thesis, İzmir Institute of Technology, Turkey (2009).
- Tadros T.F., Formulation of disperse systems: Science and Technology, John Wiley & Sons (2014).
- Al-Lami H., N. Billingham, and P. Calvert, Controlled structure methacrylic copolymers as dispersants for ceramics processing, *Chemistry of Materials*, **4(6)**, 1200 (1992).
- Farokhpay, S., A review of polymeric dispersant stabilization of titania pigment, *Advances in Colloid and Interface Science*, **151(1-2)**, 24 (2009).
- Briscoe B.J., Khan A.U., and Luckham P.F., Optimizing the alumina dispersion using commercial polyvalent electrolyte dispersants, *J. Eur. Ceram. Soc.*, **20**, 2141 (1998).
- Dhara S. and Bhargava P., Influence of nature and amount of dispersant on rheology of aged aqueous alumina gelcasting slurries, *J. Am. Ceram. Soc.*, **88**, 547 (2005).
- Mohanty S., Das B., Dhara S., Poly(maleic acid)-A novel dispersant for aqueous alumina slurry, *J. Asian Ceram.Soc.*, **1**, 184 (2013).
- Sultan M. T., Al-Lami H. S., Al-Dujiali A. H., Synthesis and characterization of alumina-grafted acrylic acid monomer and polymer and its adsorption of phenol and p-chlorophenol, *Desalination and Water Treatment*, **150**, 192 (2019).
- El-Sheikh R., Hefni H.H., El-Farargy A.F., Bekhit M., and Negm N.A., Adsorption efficiency of chemically modified chitosan towards copper and cobalt ions from industrial waste water, *Egypt. J. Chem.*, **5(3)**, 291 (2012).
- Fouda A., Hussein M.H.M., Mursy M., Hazzaa M.M., Shaban A.F. and Hefni H. H., A study on the effect of type of solvent on chitosan efficiency for treatment of drinking water contaminations, *Egypt. J. Chem.*, **63**, No. 7 (2020).
- J. Chem.*, **57(4)**, 327 (2014).
- Pellerin, N., Staley J. T., Ren T., Graff G. L., Acidic biopolymers as dispersants for ceramic processing. *Mat. Res. Soc. Symp. Proc.*, **218**, 123 (1991).
- Castro R. H., Murad B.S., Gouvêa D., Influence of the acid–basic character of oxide surfaces in dispersants effectiveness, *Ceram. Intern.*, **30(8)**, 2215 (2004).
- Hussien M.H.M. and Abdeen Z., Characterization and application of extracted natural polymer fibre (aminopolysaccharide) as weight reducing agent, *Egypt. J. Chem.*, **52(5)**, 631 (2009).
- Mutasher, S.H., Salih, A.A., Al-Lami, H.S., Preparation of some chitosan derivatives and study their effect on human genetic material, *Der Pharma Chemica*, **8(11)**, 125 (2016).
- Arafat A., Samad S. A., Masum S. Md., Moniruzzaman M., Preparation and characterization of chitosan from shrimp shell waste, *Intern. J. Sci. & Eng. Res.*, **6(5)**, 538 (2015).
- Zaboon M. H., Saleh A.A., Al-Lami H. S., Comparative cytotoxicity and genotoxicity assessments of chitosan amino acid derivative nanoparticles toward human breast cancer cell lines, *Egypt. J. Chem.*, Articles in Press, Accepted Manuscript, Available Online from 08 April 2019.
- Ilyas, S.U., PendyalaR., and MarneniN., Stability and agglomeration of alumina nanoparticles in ethanol-water mixtures, *Procedia Eng.*, **148**, 290 (2016).
- Jalal, M.A. and Al-Lami H.S., New limited molecular weight polymeric dispersants prepared by melt condensation polymerization, *Chem. Mater.*, **6(2)**, 12 (2014).
- Benns, J.M., Choi, J.S., Mahato, Park, R.I. J.S., Kim, S.W., pH-sensitive cationic polymer gene delivery vehicle: N-Ac-poly(L-histidine)-graft-poly(L-lysine) comb shaped polymer, *Bioconjug. Chem.*, **11(5)**, 637 (2000).
- Park, J.H., Saravanakumar, G., Targeted delivery of low molecular drugs using chitosan and its derivatives”, *Advance Drug Delivery Rev.*, **62**, 28 (2010).
- Huggins, M.L., The viscosity of dilute solutions of long-chain molecules. IV. Dependence on concentration, *J. Amer. Chem. Soc.*, **64**, 2716 (1942).

22. N. Yacob, N. Talip, M. Mahmud, N.A I. Sani, N.A. Samsuddin, N.A. Fabillah, " Determination of viscosity-average molecular weight of chitosan using intrinsic viscosity measurement", Bangi , 43000 KAJANG, MALAYSIA, [http://www.iaea.org/inis/collection/NCLCollectionStore/\\_Public/44/122/44122710.pdf](http://www.iaea.org/inis/collection/NCLCollectionStore/_Public/44/122/44122710.pdf).
23. Hossain, M.S., Iqbal, A., Production and characterization of chitosan from shrimp waste, *J. Bangladesh Agril. Univ.*, **12(1)**, 153 (2014).
24. Ji J., Wang L., Yu H., Chen Y., Zhao Y., Zhang H., Amer W. A., Sun Y., Huang L., Saleem M., Chemical modifications of chitosan and its applications, *Polymer-Plastics Techn. Eng.*, **53**, 1494 (2014).
25. Chou, K.S. and Lee L.J., Effect of dispersants on the rheological properties and slip casting of concentrated alumina slurry, *J. Am. Ceram. Soc.*, **72(9)**, 1622 (1989).
26. Parfitt G.D., Dispersion of powders in liquids, 2<sup>nd</sup> edition, John Wiley & Sons, New York, 1973.
27. Napper D.H., Steric stabilization, *J. Colloid Interf. Sci.*, **58**, 390 (1977).
28. Ghosh A., Ali M. A., Studies on physicochemical characteristics of chitosan derivatives with dicarboxylic acids, *J. Mater. Sci.*, **47**, 1196 (2012).
29. Foo K.Y. and Hameed, B.H., Insights into the modeling of adsorption isotherm systems. *Chem. Eng. J.*, **156(1)**, 2 (2010).
30. Tsubaki J., Kato M., Miyazawa M., Kuma T., Mori H., The effects of the concentration of a polymer dispersant on apparent viscosity and sedimentation behaviour of dense slurries. *Chem. Eng. Sci.*, **56**, 3021 (2001).
31. Langmuir I., The adsorption of gases on plane surface of glass, mica and platinum, *J. Am. Chem. Soc.*, **40**, 1361 (1918).
32. Chen X., Modeling of experimental adsorption isotherm data. *Information*, **6(1)**, 14 (2015).
33. Giles C. H., Smith D., Huitson A., A general treatment and classification of the solute adsorption isotherm, *J. Colloid. Interf. Sci.*, **47(3)**, 755 (1974).
34. Dada A.O., Olalekan A.P., Olatunya A.M., DADA O., Langmuir, Freundlich, Temkin and Dubinin–Radushkevich isotherms studies of equilibrium sorption of Zn<sup>2+</sup> onto phosphoric acid modified rice husk, *IOSR J. Appl. Chem.*, **3(1)**, 38 (2012).
35. Dubinin M.M., Zaverina E.D., Radushkevich L.V., Sorption and structure of active carbon I. Adsorption of organic vapours, *J. Phys. Chem. A*, **21**, 1351 (1947).
36. Tang X., Ripepi O., Luxbacher K., Pitcher E., Adsorption models for methane in shales: Review, comparison, and application, *Energy & Fuels*, **31(10)**, 10787 (2017).
37. Wu J., Strömqvist M. E., Claesson O., Fängmark I. E., Hammarström L., A systematic approach for modelling the affinity coefficient in the Dubinin–Radushkevich equation, *Carbon*, **40(14)**, 2587 (2002).
38. Benhammou, A., Yaacoubi A., Nibou L., Tanouti B., Adsorption of metal ions onto Moroccan stevensite: kinetic and isotherm studies. *J. Colloid Interf. Sci.*, **282(2)**, 320 (2005).
39. Bouabidi Z. B., El-Naas M. H., Cortes D., and McKay G., Steel-making dust as a potential adsorbent for the removal of lead (II) from an aqueous solution. *Chem. Eng. J.*, **334**, 837 (2018).
40. Debrassi A., Thaisa B., Demarchi C. A., Nedelko N., Ślawska-Waniewska A., Dłużewski P., Bilska M., and Rodrigues C. A., Adsorption of remazol red 198 onto magnetic N-lauryl chitosan particles: equilibrium, kinetics, reuse and factorial design, *Environ. Sci. Pollut. Res.*, **19**, 1594 (2012).
41. Li D. P., Zhang Y. R., Zhao X. X., Zhao B. X., Magnetic nanoparticles coated by aminoguanidine for selective adsorption of acid dyes from aqueous solution, *Chem. Eng. J.*, **232**, 425 (2013).
42. Chen A. H., Chen S. M., Biosorption of azo dyes from aqueous solution by glutaraldehyde-crosslinked chitosan, *J. Hazardous Mater.*, **172**, 1111 (2009).
43. Chiu C. W., Wu M.T., Lee J. C. M., and Ting-Yu Chen, Isothermal adsorption properties for the adsorption and removal of reactive blue 221 dye from aqueous solutions by cross-linked β-chitosan glycan as acid-resistant adsorbent, *Polymers*, **10(12)**, 1328 (2018).
44. Tzereme A., Christodoulou E., Kyzas G. Z., Kostoglou M., Bikiaris D. N., and Lambropoulou D. A., Chitosan grafted adsorbents for diclofenac pharmaceutical compound removal from single-component aqueous solutions and mixtures, *Polymers*, **11(3)**, 497 (2019).
45. El-Zawahry, M. M., Abdelghaffar F., Abdelghaffar R. A., Hassabo A. G., Equilibrium and kinetic models on the adsorption of reactive Black 5 *Egypt. J. Chem.* **63**, No. 7 (2020)

- from aqueous solution using Eichhorniacrassipes/chitosan composite. *Carbohydrate Polymers*, **136**,507 (2016).
46. Ebadi, A., Mohammadzadeh, J.S.S., and Khudiev A., What is the correct form of BET isotherm for modeling liquid phase adsorption. *Adsorption*, **15**(1), 65 (2009).
47. Demerger-André, S. and A. Domard, Chitosan behaviours in a dispersion of undecylenic acid. *Structural parameters. Carbohydrate Polymers*, **24**(3),177 (1994).
48. Jalal, M.A., Synthesis and Characterization of Different Molecular Weights Ethylene Glycol-Sebacic Acid Polymers and Their Use as Dispersants for Ceramic Particles. MSc Thesis, 2011, University of Basrah, Iraq.
49. Kakui T., Miyauchi T., Kamiya H., Analysis of the action mechanism of polymer dispersant on dense ethanol alumina suspension using colloidal probe AFM, *J. Eur. Ceram. Soc.*, **25**(5), 655 (2005).

### تحضير ودراسة إمتزاز بعض مشتقات الكيتوسان الحامضية كمشتتات لمسحوق الألومينا السيراميكي

إيمان سمير العلق، هادي سلمان اللامي و علي حسين الموالي  
قسم الكيمياء - كلية العلوم - جامعة البصرة - البصرة- العراق .

إن لطبيعة ووظائف الكيتوسان المختلفة اضافة أفضلية واضحة لتطبيقات البوليمرات الطبيعية، ليس فقط لغرض إعادة فصل وتركيز أيونات المعادن فحسب، بل أيضا لتشكيل طيف واسع من المواد الفعالة، وفتح نافذة جديدة لتطبيقاتها كمشتتات لدقائق السيراميك في الوسط المائي؛ ولهذا السبب ركزت الدراسة الحالية على الحصول على الكيتوسان من الكيتين المستخرج من قشور الجمبري بالطرق الكيميائية المعروفة وبدرجة إزالة أستله عالية بلغت 93٪ مما يساعد على زيادة ذوبانيته المحاليل الحامضية المائية. تم تحضير ثلاثة مشتقات كيتوسانية حامضية بتطعيم سلاسل الكيتوسان مع حامض الكلوتريك وحامض البيبيليك وحامض السيبياسيك، حيث تم التأكد من صحة التراكيب الناتجة بتقنية مطيافية الأشعة تحت الحمراء. تم تقييم قابلية الكيتوسان ومشتقاته الحامضية للعمل كمشتتات لمسحوق الألومينا السيراميكي وذلك بتقنيتي التركيب والانسيابية . أظهرت النتائج أن لهذه المشتقات قدرة تشنيتية جيدة لجسيمات الألومينا في الوسط المائي الحامضي الذي له الأولوية كوسط بالنسبة للشركات المصنعة للسيراميك.

تم تحديد كمية البوليمرات المتمزة على سطح الألومينا بطريقة التحليل الحراري الوزني وبالتالي تحديد تركيز المشتت المتبقي في حالة توازن في المحلول، وبالتالي تحديد تركيز المشتت المتبقي في حالة توازن في المحلول. درست أربعة نماذج من معاملات الإمتزاز الأيزوثيرمي وتقييمها عن طريق حساب المتغيرات والثوابت لكل نوع ودراسة سلوك البوليمرات المتمزة تجاه كل نموذج. تم الحصول على منحنى-S لعلاقة كمية البوليمر المتمز على سطح الألومينا مع تركيزه غير المتمز في حالة التوازن، واستنتج من ذلك ان الأمتزاز هو من نوع متعدد الطبقات حيث تتبع كل طبقة لايسوترم لانغموير-فرندليني.